

Theory of electromagnetic response and collective excitations of a square lattice of antidots

S. A. Mikhailov*

Institut für Theoretische Physik, Universität Regensburg, D-93040 Regensburg, Germany

(Received 13 August 1996)

An analytic theory of electromagnetic response and collective excitations of antidot superlattices is presented. Explicit functional dependencies of the response functions and the excitation spectra on the antidot lattice parameters are found. New collective modes of the system are predicted. Two-dimensional electron systems both with and without the screening metal electrodes are considered. The theory quantitatively agrees with experimental data. [S0163-1829(96)50844-1]

Lateral superlattices of antidots have been attracting increased attention because of the interesting physical phenomena recently observed in these systems. Magnetotransport experiments exhibit pronounced resistivity peaks at magnetic fields B for which the diameter of the cyclotron orbit $2r_c$ is commensurate with the lattice constant a .^{1,2} Far-infrared (FIR) transmission experiments³⁻⁷ show a characteristic two-mode behavior of the collective excitations with the upper mode converging at large B towards the cyclotron resonance (CR) $\omega = \omega_c$, and the lower, edge magnetoplasmon (EMP) mode associated with electrons skipping around each antidot. The dispersion of these modes for high magnetic fields is the same as for quantum dots. However, for $B \rightarrow 0$ the behavior is quite different. In dots upper and lower modes converge to the frequency of the dimensional plasma resonance at $B=0$. In antidots, they show an anticrossing feature with exchange of oscillator strength: the upper mode passes through the minimum and tends to a finite frequency with negative B dispersion at $B \rightarrow 0$; the lower mode passes through the maximum and linearly tends to zero with B . In addition, the weak CR line is observed between two main resonances in antidot structures.

Contrary to the dc magnetotransport in antidot superlattices and the FIR spectra of quantum dots, the excitation spectrum of antidot superlattices is not yet completely understood. The theoretical papers published so far⁸⁻¹¹ have the principal shortcoming that they did not take into account properly the periodicity of the real antidot lattice. In Ref. 8, the authors dealt with the problem of a single antidot. Wu and Zhao⁹ replaced the real (square) Wigner-Seitz cell by the circular one and solved the problem numerically. Although they obtained an agreement with experimental data,^{3,4} the dependence on antidot lattice parameters was not clarified. The results⁹ cannot therefore be used to analyze new experiments. In our previous work,^{10,11} the problem was solved in modified dipole approximation (which agrees with experiment but is valid only at $\omega < \omega_c$) and in effective medium approximation (EMA) (in which the problem of the antidot lattice was replaced by that of a single antidot immersed in an effective 2D medium). EMA, although reproducing the essential features of the experimental data, would give identical results for both a square lattice of antidots and a disordered system of randomly distributed antidots with the same area filling factor.¹¹

In this paper we present the *analytic* solution of the problem of electromagnetic response of the antidot lattice *taking fully into account* its real spatial symmetry. We obtain explicit functional dependencies of the response function of an antidot in the lattice, the macroscopic conductivity, the absorption coefficients and the excitation spectrum on the lattice constant, the antidot radius, the distance from 2DES to screening metal electrodes, and the electron density profile in antidots. We show that the full dipole excitation spectrum consists of three types of modes: the single-particle CR $\omega = \omega_c$, which is due to the "background" electrons of 2DES, the EMP mode $\omega_{\text{EMP}} < \omega_c$, and an infinite set of high-frequency modes $\omega_{m,n}^{(\pm)}(B) > \omega_c$. The EMP mode is strongly localized near the antidot boundaries;¹¹ its frequency depends mainly on the antidot radius R , but not on the lattice period a . The high-frequency modes $\omega_{m,n}^{(\pm)}$ are excited in the system due to the antidot superlattice, which can be considered as a grating coupler imposed on the homogeneous 2DES. The frequencies $\omega_{m,n}^{(\pm)}(B)$ are close to those of 2D bulk magnetoplasmons, $\omega_{\text{MP}}(\mathbf{G}_{m,n}, B)$, with the wave vectors \mathbf{q} equal to all reciprocal lattice vectors $\mathbf{G}_{m,n} = (2\pi/a)(m, n)$. The high-frequency modes $\omega_{m,n}^{(\pm)}(B)$ are the principal new result of our theory; only the mode $\omega_{1,0}^{(+)}$ has been observed so far.

Let the 2DES be placed at the plane $z=0$ between two metal electrodes at the planes $z=d_1$ and $z=-d_2$, the background dielectric constants equal to ϵ_1 at $0 < z < d_1$ and ϵ_2 at $-d_2 < z < 0$, and an equilibrium electron density of 2D electrons written as

$$n_0(\mathbf{r}) = n_0 \{1 - \Theta(\mathbf{r})\}, \quad \Theta(\mathbf{r}) = \sum_{i,j} \vartheta(\mathbf{r} - \mathbf{a}_{i,j}). \quad (1)$$

Here n_0 is the background density of a homogeneous 2DES and $\mathbf{a}_{i,j} = a(i, j)$, i, j integer, are the lattice vectors. The function $\vartheta(\mathbf{r}) \equiv \vartheta(r)$ describes the density profile near an antidot; it changes from $\vartheta(r) = 1$ inside of the antidots to $\vartheta(r) = 0$ outside of the antidots on a distance small compared to a and R . The system is probed by an external electric field, uniform and parallel to the plane $z=0$; it is described by the scalar potential $\varphi_{\text{ext}}(\mathbf{r}, t) = \varphi_{\pm}^{\text{ext}}(r) \exp(\pm i\theta - i\omega t)$, where $\varphi_{\pm}^{\text{ext}}(r) = -E_{\pm}^0 r / \sqrt{2}$ and $E_{\pm}^0 = (E_x^0 \mp iE_y^0) / \sqrt{2}$ are the field amplitudes with \pm circular

polarization. The upper sign corresponds to the polarization of the CR.

The dynamic fluctuations of the charge density $\rho(\mathbf{r}) = \sum_{\mathbf{G}} \rho_{\mathbf{G}} e^{i\mathbf{G}\cdot\mathbf{r}}$ and the induced potential φ_{ind} in the system are related by the Poisson equation with the boundary conditions $\varphi_{\text{ind}}|_{z=d_1, -d_2} = 0$. In the case of antidots, it is more relevant¹¹ to present ρ in the form $\rho = \rho^{\text{homo}} + \delta\rho$, where $\rho_{\mathbf{G}}^{\text{homo}} = G^2 \sigma_{\text{LL}}(G, \omega) \varphi_{\mathbf{G}}^{\text{tot}} / i\omega$ corresponds to the charge density fluctuations in the uniform 2DES with the density n_0 and $\delta\rho_{\mathbf{G}} = G_{\alpha} \delta j_{\alpha}^{\mathbf{G}} / \omega$ is due to the lack of electrons in antidots; here $\sigma_{\text{LL}}(G, \omega)$ is the longitudinal diagonal conductivity of the uniform 2DES and $G = |\mathbf{G}|$. The Poisson and continuity equations then give

$$E_{\alpha}^{\text{ind}}(\mathbf{r}) = \frac{2\pi}{i\omega} \sum_{\mathbf{G} \neq 0} \frac{G_{\alpha} G_{\beta} e^{i\mathbf{G}\cdot\mathbf{r}}}{G \epsilon_{\text{LL}}(G, \omega)} \delta j_{\beta}^{\mathbf{G}}, \quad (2)$$

where

$$\epsilon_{\text{LL}}(G, \omega) = [\epsilon_1 \coth(Gd_1) + \epsilon_2 \coth(Gd_2)] / 2 + 2\pi i \sigma_{\text{LL}}(G, \omega) G / \omega \quad (3)$$

is the dielectric function of the system ‘‘metal - dielectric - 2DES - dielectric - metal.’’¹² Assuming the local relation between $\delta j(\mathbf{r})$ and $\mathbf{E}^{\text{tot}}(\mathbf{r})$ we obtain

$$\delta j_{\alpha}^{\mathbf{G}} = \sigma_{\alpha\beta}(0, \omega) \langle \vartheta(r) E_{\beta}^{\text{tot}}(\mathbf{r}) e^{-i\mathbf{G}\cdot\mathbf{r}} \rangle; \quad (4)$$

the angular brackets mean the average over the area of an elementary cell.

Equations (2) and (4) relate the induced field at any point in the 2DES with the total electric field inside antidots. To solve them one has to expand the unknown functions $E_{\alpha}^{\text{ind}}(\mathbf{r})$ at $r < R$ over a set of suitable orthogonal polynomials and then to solve the resulting system of equations for expansion coefficients. We restrict ourselves to the first term in this expansion, assuming that the induced (and total) electric field *inside the antidots* is uniform, $\mathbf{E}(\mathbf{r}) = \text{const}$ at $r < R$. Then for a square lattice of circular antidots we find

$$E_{\pm}^{\text{tot}} = E_{\pm}^0 / \zeta_{\pm}(\omega, B), r < R. \quad (5)$$

Here the function

$$\zeta_{\pm}(\omega, B) = 1 - \frac{\pi i \langle \vartheta \rangle \sigma_{\pm}(\omega)}{\omega} \sum_{\mathbf{G} \neq 0} \frac{G \alpha(G)}{\epsilon_{\text{LL}}(G, \omega)} \quad (6)$$

has the meaning of the response function of one antidot in the lattice, $\sigma_{\pm} = \sigma_{xx} \pm i\sigma_{xy}$, $\langle \vartheta \rangle$ is the area filling factor, and

$$\alpha(G) = \left| \frac{\langle \vartheta e^{i\mathbf{G}\cdot\mathbf{r}} \rangle}{\langle \vartheta \rangle} \right|^2 \quad (7)$$

is a form factor determined by the Fourier components of equilibrium density profile near the antidots.

Making use of Eqs. (2), (4), and (5), one can calculate the macroscopic conductivity

$$\sigma_{\pm}^{\text{macro}}(\omega) = \sigma_{\pm}(\omega) \{1 - \langle \vartheta \rangle / \zeta_{\pm}(\omega)\} \quad (8)$$

and the absorption coefficients $\gamma_{\pm}(\omega)$ of the structure,

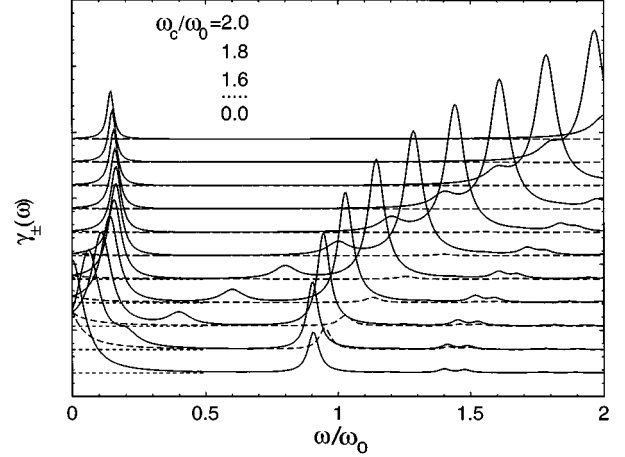


FIG. 1. The absorption coefficients $\gamma_{+}(\omega)$ (solid curves) and $\gamma_{-}(\omega)$ (dashed curves), Eq. (9), of the unscreened ($d_1 = d_2 = \infty$) square lattice of antidots at different magnetic fields, $\langle \vartheta \rangle = 0.5$ and $\omega_0 \tau = 20$.

$$\gamma_{\pm} = \sigma'_{\pm} - \frac{\langle \vartheta \rangle \sigma'_{\pm}}{|\zeta_{\pm}|^2} + \frac{\sigma'_{xx}}{2} \left| \frac{2\pi \langle \vartheta \rangle \sigma_{\pm}}{\omega \zeta_{\pm}} \right|^2 \sum_{\mathbf{G} \neq 0} \frac{G^2 \alpha(G)}{|\epsilon_{\text{LL}}(G, \omega)|^2}. \quad (9)$$

Here the prime means the real part and γ_{\pm} are defined as $Q_{\pm} = \gamma_{\pm} |E_{\pm}^0|^2 / 2$, Q is Joule's heat.

Figure 1 demonstrates the frequency dependence of the absorption coefficients $\gamma_{\pm}(\omega)$ at different magnetic fields, for $\langle \vartheta \rangle = 0.5$ and $\omega_0 \tau = 20$, where $\omega_0 \equiv \omega_p(G_{1,0})$ is the frequency of 2D bulk plasmon with the fundamental reciprocal lattice vector $G_{1,0} = 2\pi/a$, and τ is the momentum relaxation time. For simplicity we use here the local expression for the conductivity $\sigma_{\text{LL}}(G, \omega)$ of the uniform 2DES (Drude model). As pronounced features the calculated spectra of Fig. 1 show the observed resonances. In addition we find the weak - polarized mode at $\omega \approx \omega_0$ (it was predicted in Refs. 9–11) and a set of high-frequency + and - polarized modes at $\omega/\omega_0 > 1$ with smaller oscillator strengths. These new high-frequency modes were not observed or predicted till now.

The position of resonances is determined by the poles of absorption coefficients $\gamma_{\pm}(\omega)$ which coincide with (a) the poles of $\sigma_{\pm}(\omega)$ and (b) the zeros of $\zeta_{\pm}(\omega)$. The poles of $\sigma_{\pm}(\omega)$ give the *single-particle* contribution $\omega = \omega_c$ to the excitation spectrum with an oscillator strength¹³

$$S_{\text{cr}} = \left\{ 1 + \frac{\langle \vartheta \rangle^2}{\langle \vartheta \rangle - \langle \vartheta^2 \rangle} \right\}^{-1}. \quad (10)$$

In order to find the resonance frequencies of the *collective modes* [the zeros of $\zeta_{\pm}(\omega)$] we rewrite Eq. (6) using the collisionless Drude formulas for $\sigma_{\alpha\beta}(\omega)$,

$$\zeta_{\pm}(\omega) = 1 + \frac{\langle \vartheta \rangle}{2} \frac{\omega \pm \omega_c}{\omega} \sum_{\mathbf{G} \neq 0} \alpha(G) \frac{\omega_p^2(G)}{\omega^2 - \omega_{\text{MP}}^2(G)}. \quad (11)$$

Here $\omega_p(G)$ and $\omega_{\text{MP}}(G)$ are the frequencies of 2D bulk plasmons and magnetoplasmons,

$$\omega_p^2(G) = \frac{4\pi n_0 e^2 G}{m^* \{ \epsilon_1 \coth(Gd_1) + \epsilon_2 \coth(Gd_2) \}}, \quad (12)$$

$$\omega_{\text{MP}}^2(G) = \omega_p^2(G) + \omega_c^2; \quad (13)$$

m^* is the effective mass of electrons. As seen from Eq. (11), the functions $\zeta_{\pm}(\omega)$ have an infinite set of poles at $\omega = \omega_{\text{MP}}(\mathbf{G}_{m,n})$ and an infinite set of zeros at the frequencies

$$\omega_{m,n}^{(\pm)}(B) = \omega_{\text{MP}}(\mathbf{G}_{m,n}) [1 - \Delta_{m,n}^{(\pm)}(B)]^{1/2}, \quad (14)$$

which are shifted down with respect to the poles. To the first order in $\Delta_{m,n}^{(\pm)}$ one can find that

$$\frac{\Delta_{m,n}^{(\pm)}(B)}{\Delta_{m,n}} = \frac{\omega_p^2(G_{m,n}) [\omega_{\text{MP}}(G_{m,n}) \pm \omega_c]}{\omega_{\text{MP}}^3(G_{m,n})}, \quad (15)$$

$$\Delta_{m,n} \equiv \Delta_{m,n}^{(\pm)}(0) = g_{m,n} \langle \vartheta \rangle \alpha(G_{m,n})/2, \quad (16)$$

where $g_{m,n}$ is the degeneracy factor (the number of terms in the sum over \mathbf{G} with the same $m^2 + n^2$: $g_{1,0} = g_{1,1} = g_{2,0} = 4$, $g_{2,1} = 8$, etc). Oscillator strengths $S_{m,n}^{(\pm)}(B)$ of the modes $\omega_{m,n}^{(\pm)}$ are given by

$$\frac{S_{m,n}^{(\pm)}(B)}{S_{m,n}} = \frac{[\omega_{\text{MP}}^2(G_{m,n}) + \omega_c^2][\omega_{\text{MP}}(G_{m,n}) \pm \omega_c]^2}{\omega_{\text{MP}}^4(G_{m,n})}, \quad (17)$$

$$S_{m,n} \equiv S_{m,n}^{(\pm)}(0) = \langle \vartheta \rangle \Delta_{m,n}. \quad (18)$$

The slope $d\omega_{m,n}^{(\pm)}/d\omega_c$ at $B \rightarrow 0$ is determined by the same factor $\Delta_{m,n}$:

$$d\omega_{m,n}^{(\pm)}/d\omega_c|_{B=0} = \mp \Delta_{m,n}/2. \quad (19)$$

In finite B the function $\zeta_+(\omega)$ has one additional low-frequency zero $\omega_{\text{EMP}} < \omega_c$ [due to the pole $\omega = 0$, see Eq. (11)]. The EMP mode has the + polarization and the small damping in strong B . If $\omega_{\text{EMP}} \ll \omega_{\text{MP}}(G_{1,0})$, the EMP spectrum is written as

$$\omega_{\text{EMP}}(B) = (\omega_c + i/\tau)F/(1-F), \quad (20)$$

where $F(B)$ is a function of magnetic field,

$$F(B) = \frac{\langle \vartheta \rangle}{2} \sum_{\mathbf{G} \neq 0} \frac{\alpha(G) \omega_p^2(G)}{\omega_{\text{MP}}^2(G)}. \quad (21)$$

For an antidot lattice with a small $\langle \vartheta \rangle \ll 1$, the sum here can be replaced by the integral

$$F(B) \approx \frac{\langle \vartheta \rangle a^2}{4\pi} \int_0^\infty q dq \frac{\alpha(q) \omega_p^2(q)}{\omega_{\text{MP}}^2(q)}, \quad (22)$$

which depends on the antidot radius R , but not on the lattice period a . The corrections to Eq. (22) are due to the interantidot interaction; they are small at $\omega_c \gg \omega_p(1/R)$ in order of $\langle \vartheta \rangle^{3/2}$ in an unscreened 2DES ($d_1 = d_2 = \infty$) and $\langle \vartheta \rangle^2$ in a 2DES with screening electrodes. The weak dependence of the EMP frequency on the lattice constant results from the strong localization of EMP charge near the boundaries of antidots.¹¹

Figures 2(a) and 2(b) demonstrate the excitation spectrum

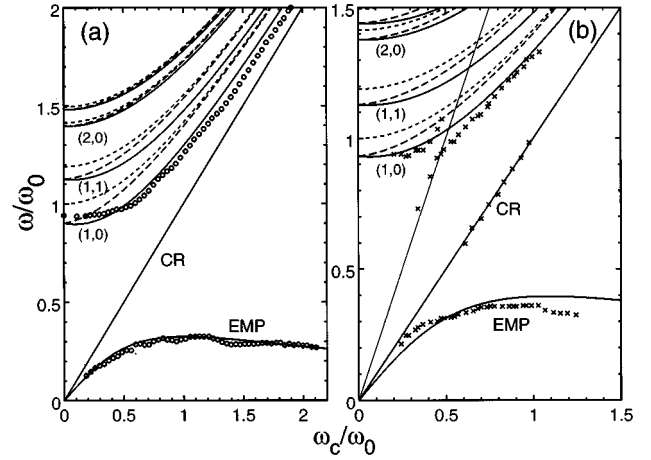


FIG. 2. The excitation spectrum of the square lattice of antidots ($d_1 = d_2 = \infty$). Solid (dashed) curves correspond to + (−) polarized modes, dotted curves to 2D bulk magnetoplasmons (13). Thin solid line in (b) is the line $\omega = 2\omega_c$. High-frequency modes $\omega_{m,n}^{(\pm)}$ are labeled by the integers $\{m,n\}$. Circles (a) and crosses (b) present the experimental data from Refs. 7 and 3, respectively.

of the antidot lattice in an unscreened 2DES ($d_1 = d_2 = \infty$) for parameters corresponding to the experimental situation in Refs. 7 and 3, respectively. Solid (dashed) curves show the + (−) polarized modes, dotted curves show the 2D bulk magnetoplasmon spectra (13). Figure 3 demonstrates the magnetic field dependence of reduced oscillator strengths of modes $\omega_{m,n}^{(\pm)}$, Eq. (17). The zero- B oscillator strengths $S_{m,n}$, Eq. (18), essentially depend on the density profile $\vartheta(r)$. We illustrate the dependence of $S_{m,n}$ on $\langle \vartheta \rangle$ for the steplike profile $\vartheta(r) = \theta(R-r)$ in the inset to Fig. 3.¹³

The circles in Fig. 2(a) and crosses in Fig. 2(b) present the experimental data from Ref. 7 (double-quantum-well $\text{Al}_x\text{Ga}_{1-x}\text{As}/\text{GaAs}$ structure with $n_0 = 9 \times 10^{11} \text{ cm}^{-2}$ in each well, $a = 800 \text{ nm}$, $R = 180 \text{ nm}$) and Ref. 3 (single-well heterostructure $\text{Ga}_x\text{In}_{1-x}\text{As}/\text{Al}_x\text{In}_{1-x}\text{As}$, $n_0 = 2.5 \times 10^{12}$

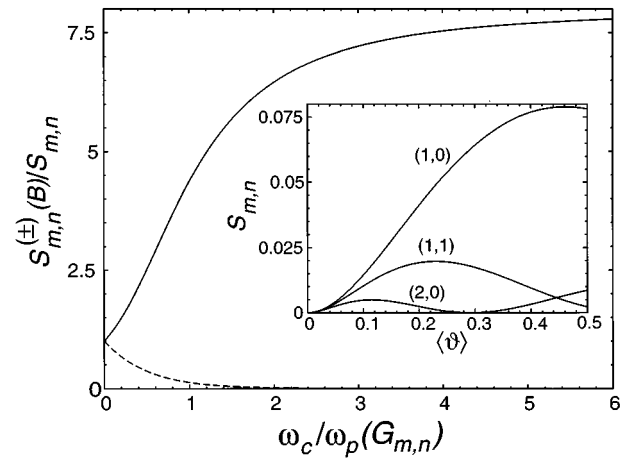


FIG. 3. The reduced oscillator strengths $S_{m,n}^{(\pm)}(B)/S_{m,n}$ of the modes $\omega_{m,n}^{(\pm)}$ (solid curve) and $\omega_{m,n}^{(-)}$ (dashed curve) as a function of reduced magnetic field $\omega_c/\omega_p(G_{m,n})$. Inset: the oscillator strengths $S_{m,n}$, Eq. (18), as a function of the area filling factor in the model of the steplike profile.

cm^{-2} , $a=300$ nm, $R=50$ nm), respectively. Apart from the value of effective mass, taken from Refs. 7 and 3, no fitting parameters was used. As seen from Fig. 2, the local theory quantitatively explains the observed excitation spectra of antidots, except the anticrossing at $\omega_{1,0}^{(+)}(B) \approx 2\omega_c$, which is seen in some experiments [Fig. 2(b)].

To describe this anticrossing, one should take into account nonlocal corrections to the conductivity of the uniform 2DES,¹⁴

$$\sigma_{\text{LL}}(G, \omega) = \frac{n_0 e^2}{m} i \omega \left\{ \frac{1}{\omega^2 - \omega_c^2} + \frac{(Gr_c/2)^2}{\omega^2 - (2\omega_c)^2} + \dots \right\},$$

$r_c \ll a$. The dispersion equation $\zeta_+(\omega) = 0$ near the intersection point then assumes the form

$$(\omega - \omega_{1,0}^{(+)}) (\omega - 2\omega_c) - \Gamma^2 = 0, \quad (23)$$

where the factor $\Gamma \approx \sqrt{3} \pi \omega_p (G_{1,0}) r_c / 4a$ determines the mode splitting at $\omega_{1,0}^{(+)} \approx 2\omega_c$.

The quantum oscillations of the EMP frequency at large B , recently observed in Ref. 7 [Fig. 2(a)], can be qualitatively understood as follows. As seen from Eqs. (20), (21),

and (7), the EMP frequency is a functional of the equilibrium electron density $\vartheta(r)$ in antidots. Effects of nonlinear screening¹⁵ should result in the B -dependent oscillations of $\vartheta(r, B)$ and hence, of the form factor $\alpha(G, B)$ and EMP frequency $\omega_{\text{EMP}}(B)$ in strong B . Note that the frequencies $\omega_{m,n}^{(\pm)}$ and the damping of the EMP and the high-frequency modes also depend on the factor $\alpha(G_{m,n}, B)$. Therefore one can expect the similar quantum oscillations of the frequency and the linewidth of *all* collective modes in the system.

In conclusion, we have developed the analytic theory of electromagnetic response of antidot superlattices which takes explicitly into account both the translational symmetry of the lattice and the circular symmetry of individual antidots. Connected with this symmetry we have predicted new modes related to the 2D magnetoplasmons. Our results are in the very good agreement with experimental data obtained in different semiconductor structures with different parameters.

I thank Professor U. Rössler, who has carefully read the manuscript and made many valuable comments, and N. Savostianova for helpful discussions. The work was supported by the Alexander von Humboldt Foundation and the NATO Science Program.

*Electronic address: sergey.mikhailov@physik.uni-regensburg.de

¹K. Ensslin and P. M. Petroff, Phys. Rev. B **41**, 12 307 (1990).

²D. Weiss, M. L. Roukes, A. Menschig, P. Grambow, K. von Klitzing, and G. Weimann, Phys. Rev. Lett. **66**, 2790 (1991).

³K. Kern, D. Heitmann, P. Grambow, Y. H. Zhang, and K. Ploog, Phys. Rev. Lett. **66**, 1618 (1991).

⁴Y. Zhao, D. C. Tsui, M. Santos, M. Shayegan, R. A. Ghanbari, D. A. Antoniadis, and H. I. Smith, Appl. Phys. Lett. **60**, 1510 (1992).

⁵A. Lorke, J. P. Kotthaus, and K. Ploog, Superlattices Microstruct. **9**, 103 (1991).

⁶A. Huber, I. Jejina, H. Lorenz, J. P. Kotthaus, S. Bakker, and T. M. Klapwijk, Semicond. Sci. Technol. **10**, 365 (1995).

⁷K. Bollweg, T. Kurth, D. Heitmann, V. Gudmundsson, E. Vasiliadou, P. Grambow, and K. Eberl, Phys. Rev. Lett. **76**, 2774 (1996).

⁸V. Fessatidis, H. L. Cui, and O. Kühn, Phys. Rev. B **47**, 6598 (1993).

⁹G. Y. Wu and Y. Zhao, Phys. Rev. Lett. **71**, 2114 (1993).

¹⁰S. A. Mikhailov and V. A. Volkov, Phys. Low-Dimens. Struct. **1**, 31 (1994).

¹¹S. A. Mikhailov and V. A. Volkov, Phys. Rev. B **52**, 17 260 (1995).

¹²See, e.g., V. A. Volkov and S. A. Mikhailov, in *Modern Problems in Condensed Matter Sciences*, edited by V. M. Agranovich and A. A. Maradudin (North-Holland, Amsterdam, 1991), Vol. 27.2, Chap. 15, p. 855.

¹³Oscillator strengths are normalized so that $S_{\text{cr}} = 1$ in the homogeneous electron layer ($\langle \vartheta \rangle = 0$).

¹⁴K. W. Chiu and J. J. Quinn, Phys. Rev. B **9**, 4724 (1974).

¹⁵V. G. Burnett, A. L. Efros, and F. G. Pikus, Phys. Rev. B **48**, 14 365 (1993).